Initial Laboratory and Sky Testing Results for the Second Generation H4RG-10 4k x 4k, 10 micron visible CMOS-Hybrid Detector

Bryan N. Dorland*[a], Rachel P. Dudik[a], Dan Veillette[a], Ryan Swindle[b], Augustyn Waczynski[c], Emily Kan[c]

[a]United States Naval Observatory, 3450 Massachusetts Avenue NW, Washington, DC 20392;
[b]Institute for Astronomy, University of Hawaii, Honolulu, HI 96822;
[c]Global Science and Technology, Inc., 7855 Walker Drive, Suite 200, Greenbelt, MD 20770 and Code 553, Goddard Space Flight Center, Greenbelt, MD 20771

ABSTRACT

We present the initial performance test results for the H4RG-10 (A2), the second generation of the H4RG-10 visible CMOS-Hybrid Sensor Chip Assembly (SCA). The first science grade H4RG-10 (A2), delivered in 2009, is an evolution of the first generation A1, first delivered and tested in 2007. The H4RG-10 is primarily intended for ground- and space-based astronomical applications. Our evaluation focused on the performance parameters as they are related to *astrometric* applications. We find that the A2 SCA shows high pixel interconnectivity (99.6%), and low read noise (10-15 e- RMS) when operated at high speeds, consistent with A1 results. Most importantly, the H4RG-10 (A2) shows a dramatic improvement in dark current vs. the A1, with a two order of magnitude reduction in mean dark level and significantly reduced hot pixel population below 200 K.

Keywords: CMOS-Hybrid, performance testing, astrometric testing

1. INTRODUCTION

The United States Naval Observatory (USNO) Astrometric Satellite Division has been engaged in a long-term effort to develop and test advanced detectors for use in both space- and ground-based astronomy, with *astrometric* applications (i.e., the measurement of position and motions of stars) being the primary focus. Development and evaluation activities have included CCDs [1], CMOS [2] and CMOS-Hybrid [3] detectors.

In 2007, USNO procured and tested first-generation, science and engineering grade H4RG-10 Sensor Chip Assemblies (SCAs) from Teledyne Imaging Sensors (TIS). The H4RG-10 is a large format (4196 x 4196 pixels) CMOS-Hybrid detector/readout sensor. The goal of the H4RG-10 development is to produce a visible/near IR (VNIR) SCA that provides the flexibility and radiation hardness of CMOS ROICs while approaching the performance of scientific grade CCDs that currently dominate the space astronomy field.

The H4RG-10 (A1) (henceforth: A1) showed significant promise for use in astronomy. As reported by Dorland et al. in more detail in ref. [3], the A1 achieved a *pixel interconnectivity* of 99.8% (i.e., 99.8% of the pixels showed high levels of response to light, indicating good connectivity between the detector pixel and the ROIC); quantum efficiency (QE) and fill factor (FF), with the QE*FF product exceeding 90% in the peak response region (approximate photometric R band); and low read noise of between 5 and 10 e- RMS after off-chip correlated double sampling (CDS) at temperatures in the 100—130K range. On the other hand, the A1 exhibited high levels of dark current, with a mean level of 30—40 e-/pixel/second at 193K as opposed to a goal of 1 e-/pix/sec. In addition, the detector showed an excessively high population of "hot" pixels (i.e., pixels that exceed a Gaussian distribution at a statistically significant level). Both of these latter effects conspired to limit the performance of the A1 for astrometry in particular, and for astronomy in general.

* email: bdorland@usno.navy.mil

Astronomical and Space Optical Systems, edited by Penny G. Warren, Cheryl J. Marshall, Robert K. Tyson, Michael Lloyd-Hart, James B. Heaney, E. Todd Kvamme, Proc. of SPIE Vol. 7439, 74390E · © 2009 SPIE · CCC code: 0277-786X/09/$18 · doi: 10.1117/12.827037

Report Documentation Page

Form Approved
OMB No. 0704-0188

1. REPORT DATE	2. REPORT TYPE	3. DATES COVERED
2009		**00-00-2009 to 00-00-2009**

4. TITLE AND SUBTITLE	5a. CONTRACT NUMBER
Initial Laboratory And Sky Testing Results For The Second Generation H4RG-10 4k x 4k, 10 Micron Visible CMOS-Hybrid Detector	5b. GRANT NUMBER
	5c. PROGRAM ELEMENT NUMBER
6. AUTHOR(S)	5d. PROJECT NUMBER
	5e. TASK NUMBER
	5f. WORK UNIT NUMBER
7. PERFORMING ORGANIZATION NAME(S) AND ADDRESS(ES) **United States Naval Observatory,3450 Massachusetts Ave, NW,Washington,DC,20392**	8. PERFORMING ORGANIZATION REPORT NUMBER
9. SPONSORING/MONITORING AGENCY NAME(S) AND ADDRESS(ES)	10. SPONSOR/MONITOR'S ACRONYM(S)
	11. SPONSOR/MONITOR'S REPORT NUMBER(S)

12. DISTRIBUTION/AVAILABILITY STATEMENT
Approved for public release; distribution unlimited

13. SUPPLEMENTARY NOTES
Proceedings of the SPIE, Volume 7439, pp. 74390E-74390E-10 (2009)

14. ABSTRACT
We present the initial performance test results for the H4RG-10 (A2), the second generation of the H4RG-10 visible CMOS-Hybrid Sensor Chip Assembly (SCA). The first science grade H4RG-10 (A2), delivered in 2009, is an evolution of the first generation A1, first delivered and tested in 2007. The H4RG-10 is primarily intended for ground- and space-based astronomical applications. Our evaluation focused on the performance parameters as they are related to astrometric applications. We find that the A2 SCA shows high pixel interconnect (99.6%), and low read noise (10-15 e- RMS) when operated at high speeds, consistent with A1 results. Most importantly, the H4RG-10 (A2) shows a dramatic improvement in dark current vs. the A1, with a two order of magnitude reduction in mean dark level and significantly reduced hot pixel population below 200 K.

15. SUBJECT TERMS

16. SECURITY CLASSIFICATION OF:			17. LIMITATION OF ABSTRACT	18. NUMBER OF PAGES	19a. NAME OF RESPONSIBLE PERSON
a. REPORT **unclassified**	b. ABSTRACT **unclassified**	c. THIS PAGE **unclassified**	**Same as Report (SAR)**	**10**	

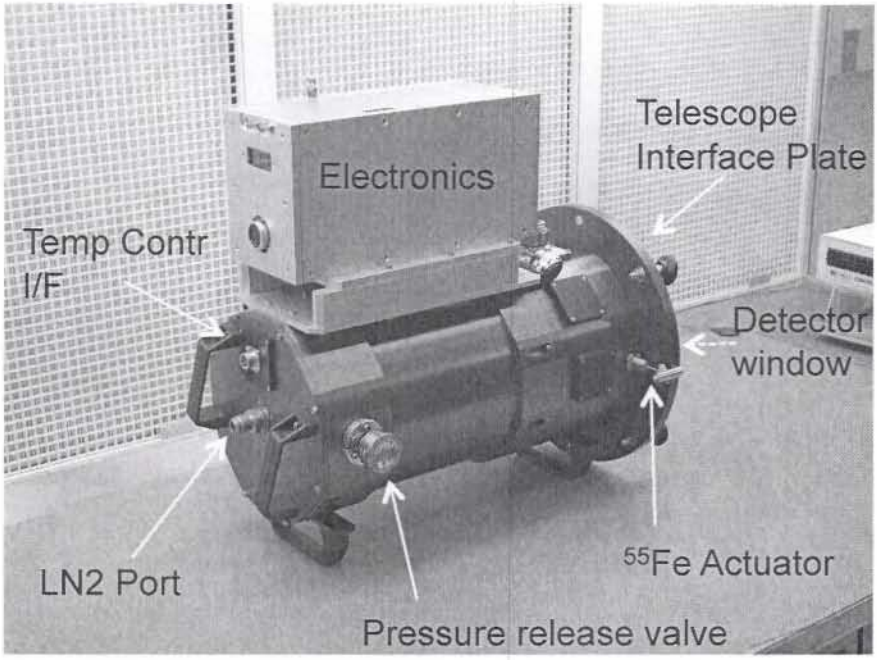

Figure 1. Ground test camera, built to support A1 testing and used for A2 testing reported in this paper.

2. H4RG-10 (A2) DEVELOPMENT

Based on the results for the A1, USNO, NASA/Goddard Space Flight Center (GSFC) and other interested parties formed a loose "consortium" to pool resources and provide direction for a second generation SCA, the H4RG-10 (A2). The primary goal of A2 development was to address the dark current and hot pixel problems associated with the A1. Working with TIS, this development consortium took delivery of second generation ROICs in 2008. These ROICs showed significant reduction in dark. USNO funded the development of full A2 hybrid SCAs, and took delivery of these in April, 2009. The remainder of this paper describes the preliminary test results for the first science grade A2 SCA.

2.1 Description of H4RG-10 (A2) and Ground Test Camera (GTC)

The H4RG-10 (A2) consists of a silicon (Si) ROIC layer bump bonded to a 100-micron thick Si "HyViSi" detector layer via indium bump bonds. The array consists of 4096 x 4096 10 micron (square) pixels. The A2 includes 64 output channels for reading out data. The ROIC supports non-destructive read, random access pixel read, random access pixel reset and windowing.

The high-speed, low-noise, cryogenic Ground Test Camera (GTC) (see Figure 1) used for this testing was originally built by GSFC's Detector Characterization Laboratory (DCL) for the A1. It consists of Leach readout, digitization and control electronics (modified to support application specific operational parameters, including high detector bias voltage), a Universal Cryogenics dewar with a hold time of at least 8 hours, a supporting data acquisition computer, temperature controller and an ^{55}Fe actuator system for gain measurements (this latter system is removed during sky testing). The interface plate is designed to allow the camera to be attached to either of the Naval Observatory, Flagstaff Station (NOFS) 1.3 m or 1.55 m telescopes. The GTC supports both lab and sky testing, allowing the FPA to be operated at temperatures of between 105 and 300K, with a stability of less than 10 mK (typical temperature stability is closer to 1-2 mK during actual use). The GTC supports "drop-in" operations of A2 ROICs and SCAs. Figure 2 shows the A2 detector in place in the GTC during the recent deployment to NOFS.

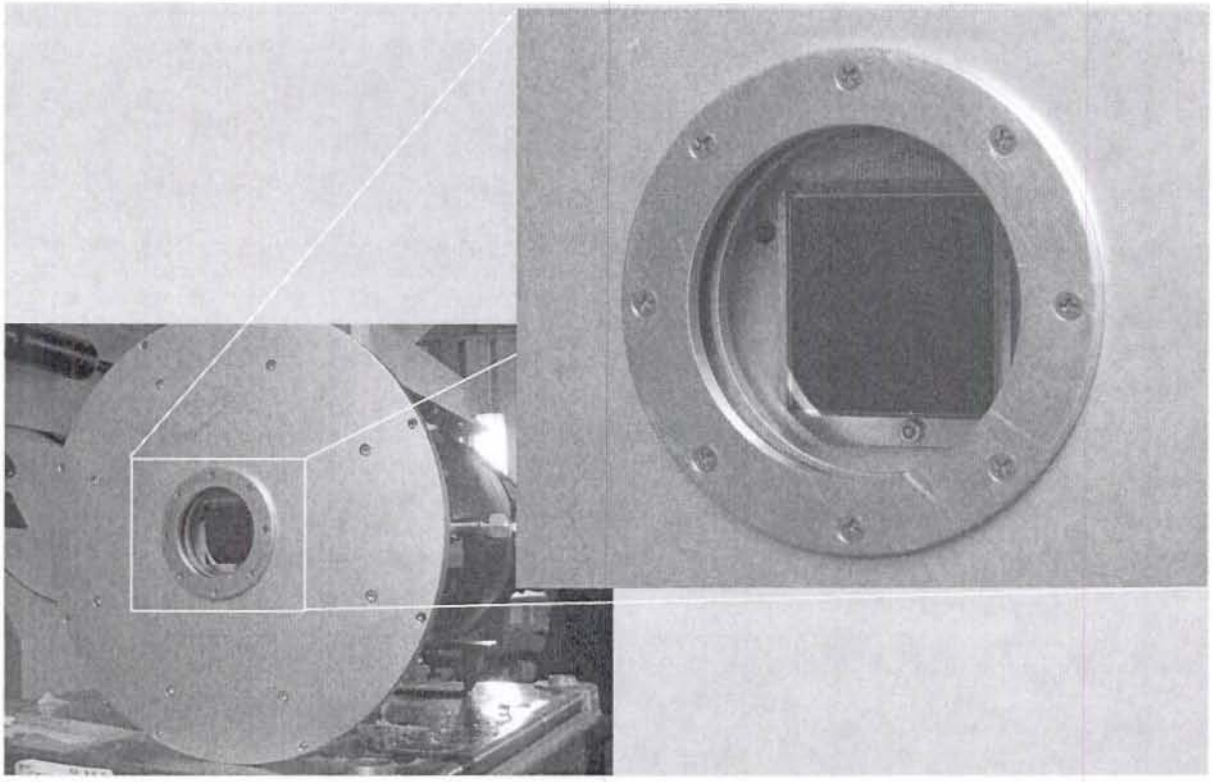

Figure 2. H4RG-10 (A2) SCA in Ground Test Camera.

3. LABORATORY TESTING

The engineering and science grade A2 units were tested at GSFC between April and June of 2009. The camera, with the science grade SCA in place, was then transported to USNO for pre-deployment operations and testing in June and July 2009. Figure 3 shows the camera undergoing flat-field testing in the USNO astrometric calibration lab.

Detector operating parameters were based on the results from A1 testing [3]. Specifically, a higher detector bias voltage (40 V) was used than is recommended in the H4RG-10 manual (15 V). This higher voltage results in over-depletion of the detector and significantly reduced electron diffusion in the detector. Higher voltages yield tighter point spread functions (PSFs) and smaller regions of electron "spillage" from hot pixels. In addition, reset voltages were varied in an attempt to linearize the dark current over differing integration times.

Initial test results are presented in the following subsections.

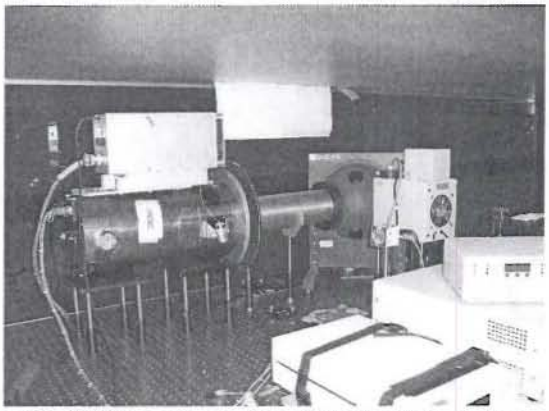

Figure 3. USNO astrometric calibration lab during H4RG-10 (A2) testing. Dewar is connected to integration sphere using stand-off baffle.

3.1 Read noise

Read noise was measured by resetting the FPA, then reading out a sequence of full-frame "images" under conditions of no illumination without resetting. These images were sequentially differenced, i.e., $image_2 - image_1$, $image_3 - image_2$, ..., $image_n - image_{n-1}$. The resultant differenced images are CDS-corrected. A Gaussian was fit to the distribution of each differenced frames and the standard deviation calculated. The read noise is given by the standard deviation of the calculated Gaussian fit for the specific differenced image. The final value for read noise was calculated by taking the mean read noise over all difference frames. The process was repeated over a range of temperatures from 130 to 230 K. Results are shown in Figure 4.

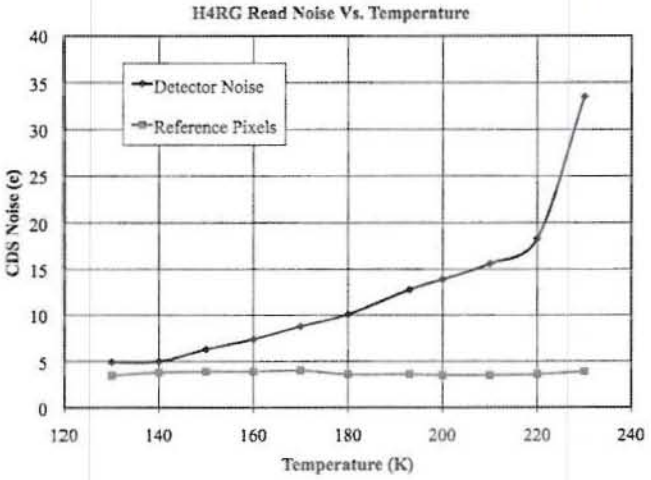

Figure 4. Read noise vs. temperature. Results shown for both detector and reference pixels.

Read noise measurements at the cold end are consistent with read noise measurements from the H4RG-10 (A1) first generation SCAs. The A2 SCAs were cooled to 110-140K in order to suppress dark current and obtain meaningful read noise measurements.

Figure 4 shows read noise for both detector and reference pixels. Above about 140K, the pixels connected to the detector show a linear increase in read noise as temperature increases, while the reference pixels do not. We speculate that the PIN material contains traps with release time constants comparable to the readout at temperature close to 190K: They are frozen at 130K and below but they become active as temperature increases. The effect probably disappears at higher temperature but cannot be easily verified due to high dark current. It would be of interest to investigate persistence as a function of temperature to see if this can be confirmed. The results are consistent with the observation that the multiplexer read noise is independent of temperature and that the detector layer is responsible for the excess, temperature-dependent noise.

3.2 Pixel operability

Pixel operability was measured by collecting flat field data. The FPA was exposed to a source of uniform illumination below saturation level and the resulting image was read out. A typical distribution is shown in Figure 5.

We observe three types of pixels: first, the vast majority (99.6%) are what we term "fully functioning." These are responsive at the 85% or higher level vs. the mean response of the SCA when illuminated by a uniform source.

A second class of pixels, labeled in the plot as "Type A" bad pixels, represents 0.26% of the array, or approximately 44 kpix out of 16.7 Mpix. These showed extremely low levels of response to input signal. These pixels appear to be disconnects where the detector pixel did not properly connect to the ROIC pixel during hybridization.

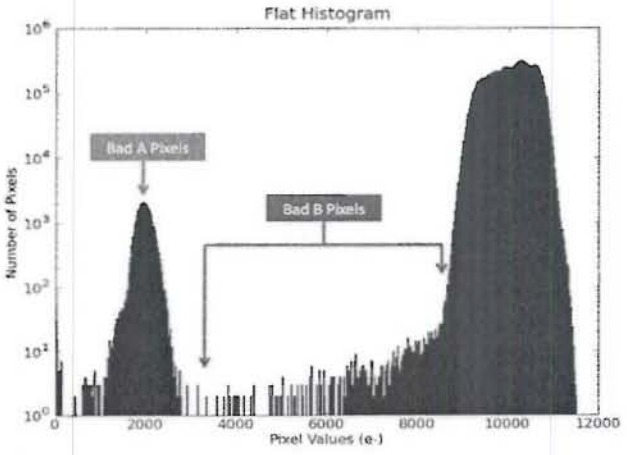

Figure 5. Distribution of pixel response to flat field illumination. Reduced responsivity is used as a diagnostic for pixel operability.

A third class of pixels, "Type B" in the plot, consists of pixels with significantly reduced response, but which are not completely disconnected. They represent 0.14% of the array, or approximately 23 kpix out of 16.7 Mpix. These pixels tend to be spatially correlated in the lower portion of the detector, and there is some evidence of MTF degradation (see discussion in section 4). The actual population affected by these pixels may be higher based on the astrometric results; future efforts will focus on better quantifying the number and nature of these pixels.

3.3 Linearity

SCA linearity was measured by allowing the SCA to integrate over many seconds while exposed to a flat field illumination source. The SCA was non-destructively read out every 1.5 seconds while charge accumulated. A best-fit line was calculated using the exposure times that are clearly not saturated. The results are shown in Figure 6.

As shown in the figure, the SCA response is highly linear over the range 0—30,000 counts, with fit residuals at the 2% level.

Configuration-specific limitations (e.g., operation in unbuffered mode) with this particular camera limit the effective full well to about 30,000 counts. Based on conversion gain measurements and known voltage swings, the detector should be able to support an effective full well capacity in excess of 100k e-.

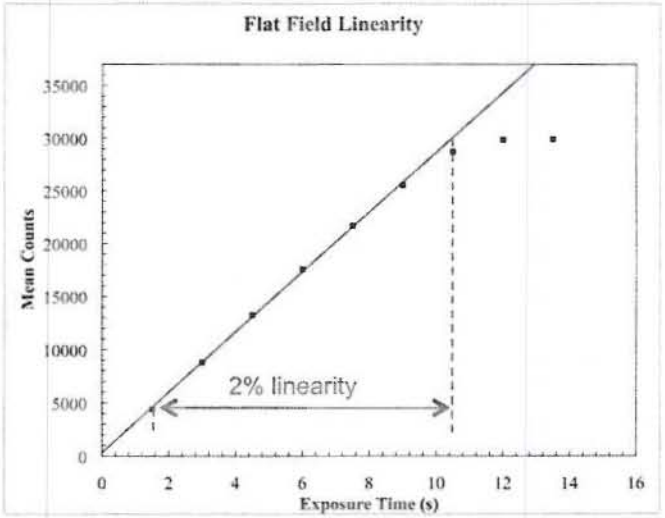

Figure 6. Linearity measurements along with best-fit line over unsaturated region.

3.4 Flat-field

As previously discussion, observation of flat-field data was critical to pixel operability and linearity measurements. In addition, flat field correction is a standard processing step for astronomical imagery; thus, it is important to understand the variations in sensitivity of the A2. Figure 7 is a sample flat field measurement.

The SCA pixels are responsive to $\leq$ 4% of the mean. The two regions with pixel connectivity problems (see section 3.2) are highlighted. The Type A bad pixels are preferentially correlated in the upper left region of the SCA, while the Type B pixels appear predominantly in the lower right, near the edge. The column striping appears to be related to the readout process, with bright stripes appears at that boundaries of two adjacent output channel regions. The diagonal marks appear to be related to the SCA fabrication process; similar marks have been seen by the authors on other Hawaii-type SCAs.

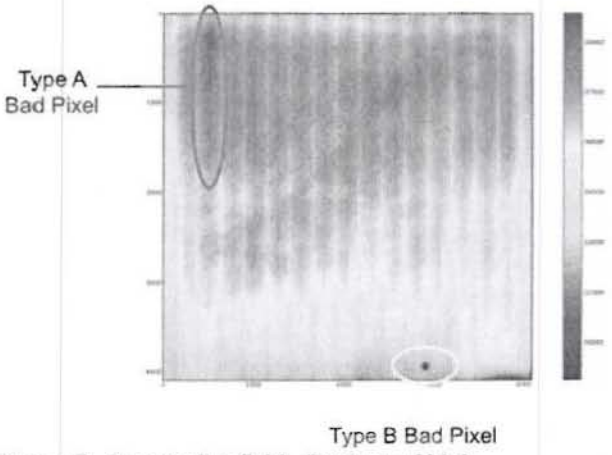

Figure 7. Sample flat field. Regions of high concentrations of bad pixels are noted. SCA is uniform at the $\leq$ 4% level.

3.5 Dark current

The previous measurements were considered necessary but not sufficient criteria for defining the A2 development successful. The *sine qua non* is significantly reduced dark current, specifically, the mean level and relative number of hot pixels. In this section, we discuss each in turn.

Mean dark current

Dark current was measured in a fashion similar to read noise (see section 3.1), with the exception that the intervals between reads used for differencing was 4.5 minutes. This served to isolate dark current from other effects such as residual bias levels. The measurements were made over a temperature range spanning 130—230 K. Results are shown in Figure 8.

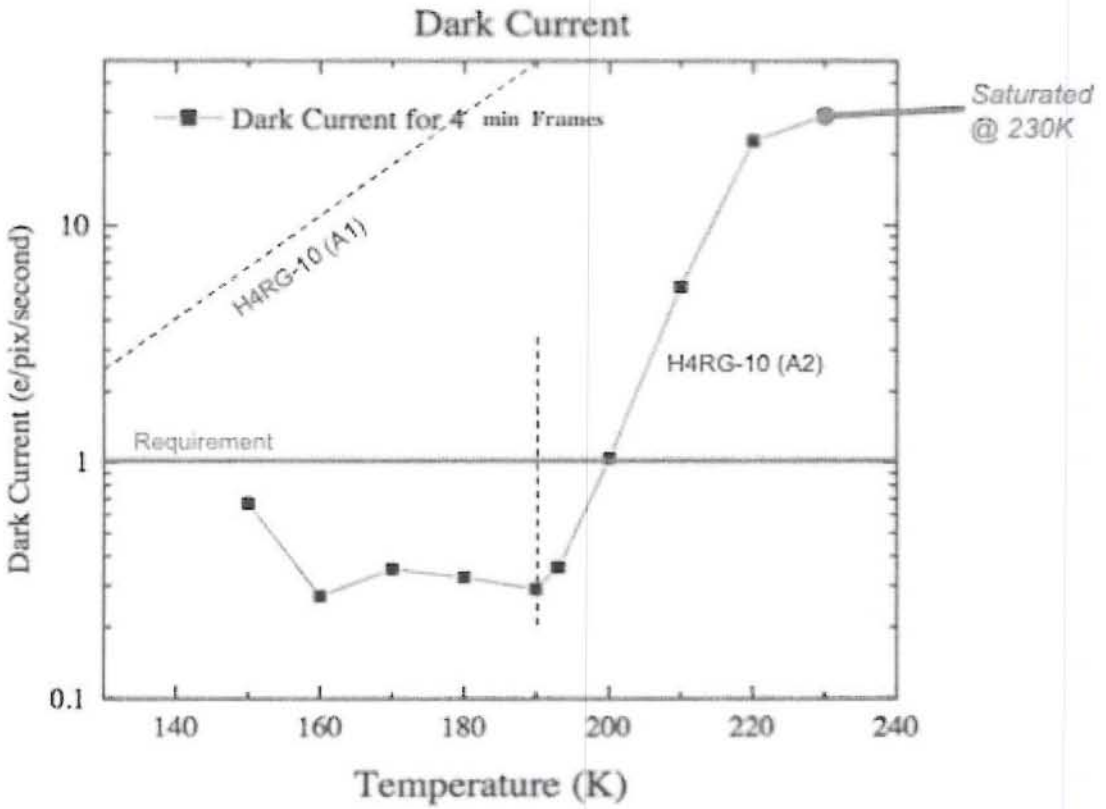

Figure 8. A2 mean dark current as a function of temperature; 4.5 minute exposures. Results from A1 are also shown as a dashed red line.

Results from both first and second generation H4RG-10 SCAs are shown in the figure. A1 results are shown as a dashed red line; A2 results are shown as a solid grey line connecting data points. The A2 showed significant reduction in mean dark current vs. the A1—approaching two orders of magnitude at typical operating temperatures of ~ 190 K. At these temperatures, the A2 exhibited mean dark currents of 0.3 e-/pixel/sec. Above this temperature, dark current increases as expected--exponentially with temperature (note that in the figure, measurements above about 30 e-/sec/pix are saturated). Below 190 K, the dark current does not appear to decrease, though the levels

were sufficiently low that these results are suspect. Additional measurements are needed to accurately measure low levels of dark current below 190K.

Dark distribution

Histograms of the distribution for three temperatures (170, 190, and 210 K) are shown in Figure 9. The distributions show that the population of hot pixels is well-behaved below about 200 K, compared with the A1 generation of detectors. At 190K the distributions is nearly Gaussian, with the population of "hot pixels" representing less than 1% of all pixels. Here we define hot pixels as those having values greater than three-sigma above the mean of the distribution. Above 200 K, an increasingly large tail of hot pixels develops. The sharp drop off of this tail is due to hot pixels that have saturated at the three-minute exposure time. These results represent a significant improvement over the A1, especially at colder (< 200 K) temperatures.

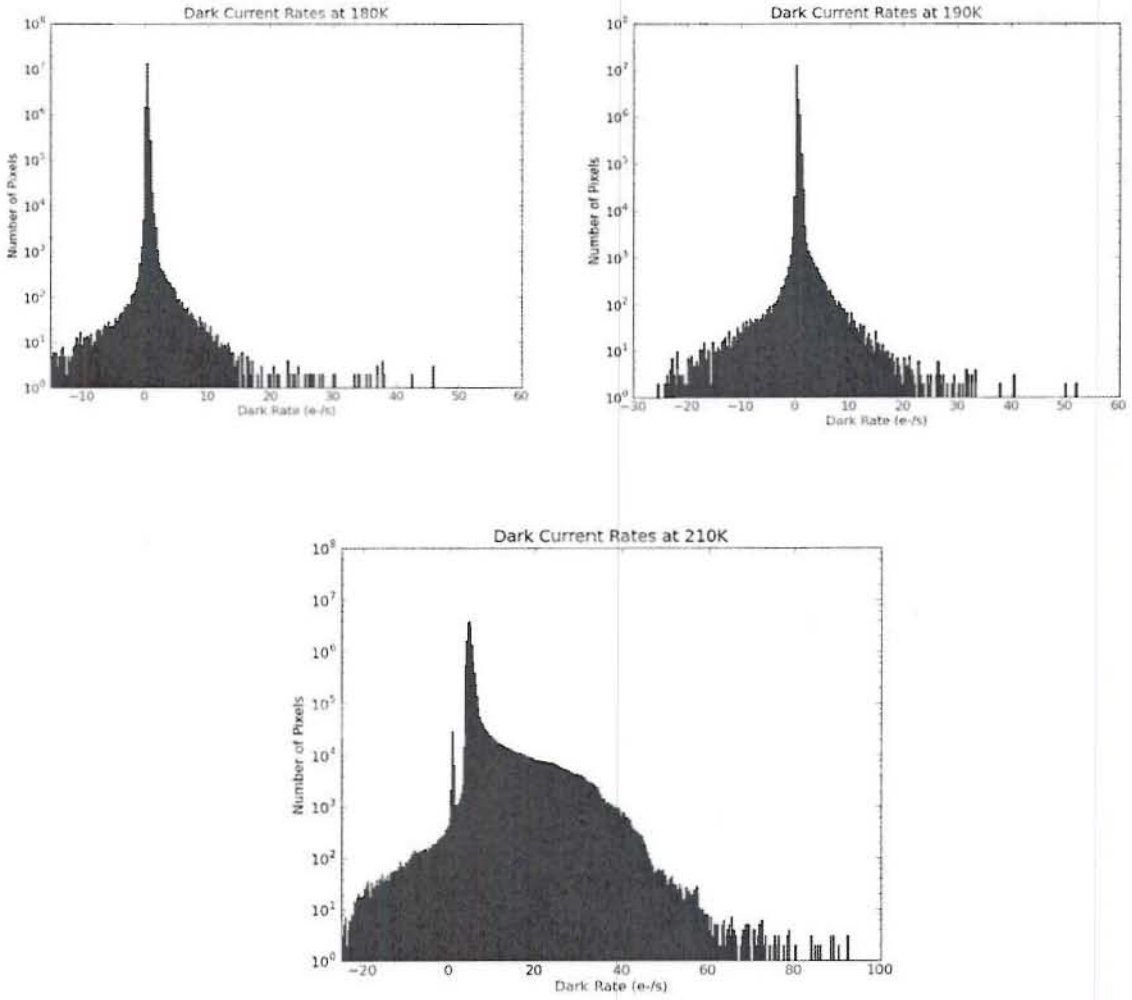

Figure 9. Dark current distributions for three temperatures.

4. ASTROMETRIC TESTING

After completion of the initial round of laboratory testing, the camera was taken to NOFS for sky testing. NOFS is the US Navy's dark sky astronomical observing site. NOFS maintains multiple telescopes for a variety of purposes, including visible and infrared camera testing and characterization.

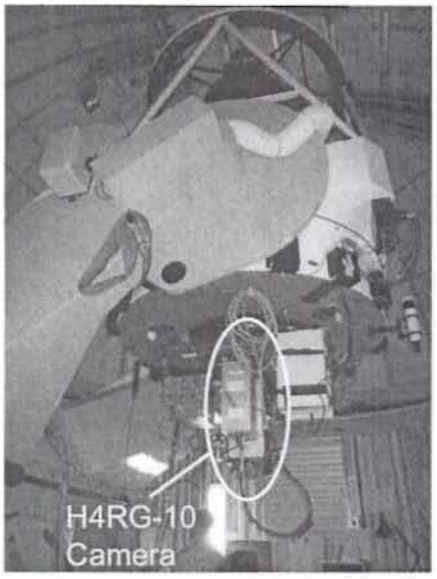

Figure 10. NOFS 1.3 m telescope with H4RG-10 camera attached.

The A2 was tested on the NOFS f/4.1, 1.3 m astrometric reflector. The telescope is shown in Figure 10. It includes a filter box with standard astronomical photometric filters as well as specialized spectrophotometric gratings. The telescope is used both with large, dedicated visible and IR astronomical cameras as well as with external test cameras such as our H4RG-10 camera.

Despite being deployed during the monsoon season, over the course of a week, we were able to collect astrometric and photometric observations of numerous astronomical objects, including M13, the Great Cluster in the constellation Hercules, M31, the Andromeda Galaxy and the open cluster M52. Figure 12 is a first-look image of M13.

4.1 Astrometric Results (first look)

In order to assess the astrometric potential of the detector, the Single Measurement Precision (SMP) systematic floor must be determined. The methodology for this assessment is as follows. Repeated observations of a relatively dense target was made over a relatively short period of time. For the presented analysis, we took four 146 second exposures of the open cluster NGC 7092 over a 1.5 hour period. Centroids of specific reference stars were calculated for each image and the results were correlated over the four images. An Affine transformation was then used to extract the translations and rotation angles of the centroids in three offset images relative to a common reference image. The standard deviation in the transformed position offsets was then calculated for each star over all four images. Each standard deviation measurement was plotted as a function of instrumental magnitude. The initial results are shown in Figure 11.

Initial astrometric results showed errors no lower than 25—30 mas. This is significantly higher than the expected ~ 10 mas from uncorrected atmospheric and telescope effects. After exclusion of the lower 20% of the detector, the results in Figure 11 were obtained. An astrometric "sweet spot" is shown between instrumental magnitudes -15 and -13 with astrometric precision in the 8—9 mas range, consistent with other sources of error. This sets an astrometric upper limit of approximately 1/70th of a pixel for the level of astrometric measurement precision supported by the SCA. As shown in the figure, stars brighter than this range saturate, with increased error; similarly, stellar centroids below this range are dominated by low signal-to-noise, leading to increased error.

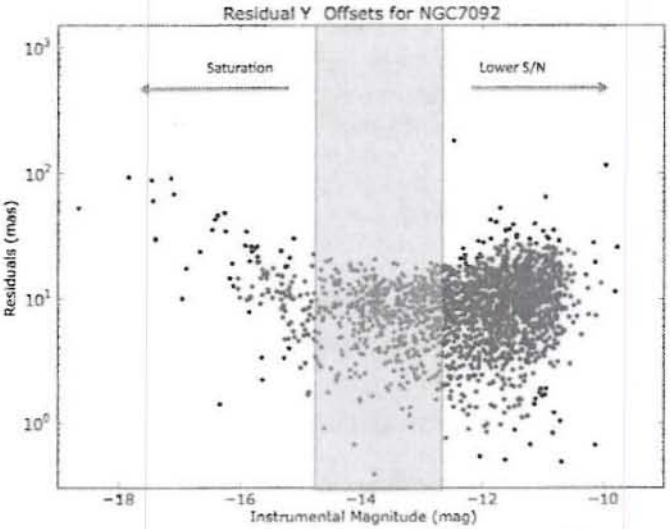

Figure 11. Single measurement precision centroiding residuals vs. instrumental magntiudes for NGC 7092. Offset to apparent magnitudes is approximately +25.

Figure 12. H4RG-10 (A2) first light image. Great Cluster in Hercules as observed through 1.3 m NOFS reflector.

Exclusion of the lower 20% of the detector was done after close inspection of PSFs revealed an overabundance of artifacts in this region, shown in Figure 7 as the area of reduced responsivity along the lower edge of the SCA. There appears to be some sort of charge sharing occurring among some pixels in this area, though the exact nature and cause is not currently understood. Additional testing and analysis will focus on understanding these effects.

5. SUMMARY

The H4RG-10 (A2) second generation CMOS-Hybrid SCA has been built and delivered to USNO, where an initial set of tests has been completed. The SCA shows good levels of pixel interoperability, low read noise and good linearity over the entire dynamic range. Most importantly, a two order of magnitude reduction in dark current has been measured, validating the design and process changes associated with the H4RG-10 (A2). This marked

improvement significantly increases the usefulness of this technology for both ground- and space-based applications.

6. FUTURE WORK

Performance testing of the A2 will continue at USNO, GSFC and the Naval Research Laboratory (NRL). Additional deployments will be made to NOFS in order to fully characterize the performance of the A2 for astrometric, photometric and spectrophotometric applications. Radiation testing of the A2 will also be performed. These results will be presented at future meetings.

In addition, design and development of a third generation SCA, the B0 has begun. Results from the A2 tests will help direct B0 development over the next year.

ACKNOWLEDGMENTS

The authors would like to acknowledge the critical support provided for these observations by the staff at the Naval Observatory Flagstaff Station (NOFS), including, but not limited to Dr. Marc Murison, Mike DiVittorrio, Fred Harris, Mike DiVitorrio, Mike Schultheis, Al Rhodes, Trudy Tilleman, and Dr. Paul Shankland. We would also like to acknowledge the contribution and help of Dr. Bernard Rauscher of Goddard Space Flight Center who formed the H4RG-10 development consortium that developed the H4RG-10 (A2) ROICs. We would like to thank Dr. Laddawan Miko, Peter Shu, Brent Mott and the staff of Goddard Space Flight Center's Detector Characterization Lab for their support in the development, maintenance and deployment of the test camera and SCAs. Finally, we would like to thank Dr. Jim Waterman of the Naval Research Lab's Optical Science Division for continued assistance in the development of the H4RG-10 and supporting technology.

REFERENCES

1. Dorland 2004, "Modeling the effects of proton damage to CCDs on astrometric measurement precision," Proc. SPIE, 5167, 302
2. Dorland, B. N. et al. 2007, "Astrometric sky testing results for the TIS 5-micron 3T-class CMOS detector," Proc. SPIE 6690-19
3. Dorland, B. N. et al. 2007, "Laboratory and Sky Testing Results for the TIS H4RG-10 4k x 4k, 10 micron visible CMOS-Hybrid Detector," Proc. SPIE 6690-13
4. Zacharias, N. 1996, "Measuring the Atmospheric Influence on Differential Astrometry: A Simple Method Applied to Wide Field CCD Frames," Publications of the Astronomical Society of the Pacific, 108, 1135